Rock and Soil Mechanics

Volume 42 | Issue 7 Article 9

11-23-2021

Analysis of laterally-loaded piles embedded in multi-layered soils using efficient finite-element method

Hai-peng ZHAO
School of Civil Engineering, Sun Yat-Sen University, Guangzhou, Guangdong 510275, China

Xue-you LI
Southern Marine Science and Engineering Guangdong Laboratory (Zhuhai), Zhuhai, Guangdong 519082, China, lixueyou@mail.sysu.edu.cn

Jian-hong WAN
School of Civil Engineering, Sun Yat-Sen University, Guangzhou, Guangdong 510275, China

Xiang-zhi ZHENG
School of Civil Engineering, Sun Yat-Sen University, Guangzhou, Guangdong 510275, China

See next page for additional authors

Custom Citation
ZHAO Hai-peng, LI Xue-you, WAN Jian-hong, ZHENG Xiang-zhi, LIU Si-wei, . Analysis of laterally-loaded piles embedded in multi-layered soils using efficient finite-element method[J]. Rock and Soil Mechanics, 2021, 42(7): 1995-2003.

Analysis of laterally-loaded piles embedded in multi-layered soils using efficient finite-element method

Authors
Hai-peng ZHAO, Xue-you LI, Jian-hong WAN, Xiang-zhi ZHENG, and Si-wei LIU

Rock and Soil Mechanics 2021 42(7): 1995–2003
https: //doi.org/10.16285/j.rsm.2020.6763
ISSN 1000–7598
rocksoilmech.researchcommons.org/journal

Analysis of laterally-loaded piles embedded in multi-layered soils using efficient finite-element method

ZHAO Hai-peng[1], LI Xue-you[1, 2], WAN Jian-hong[1], ZHENG Xiang-zhi[1], LIU Si-wei[3]

1. School of Civil Engineering, Sun Yat-Sen University, Guangzhou, Guangdong 510275, China
2. Southern Marine Science and Engineering Guangdong Laboratory (Zhuhai), Zhuhai, Guangdong 519082, China
3. Department of Civil and Environmental Engineering, The Hong Kong Polytechnic University, Hong Kong 999077, China

Abstract: Mechanical analysis of laterally-loaded piles embedded in multi-layered soils is a critical step in design. Traditional finite-element method may have deficiency in accuracy and efficiency when applied to analyze this problem. An efficient finite-element method is proposed in this paper. A “pile element” that adopts the distributed “soil springs” along the element length to reflect the nonlinear behaviors of the pile-soil interactions is developed in this method. The dominant feature of the pile element is the direct integration of soil properties into the element formulation, namely, a pile element comprises both the pile and soil properties. The pile element formulation in multi-layered soils is derived, and the Gauss-Legendre method is introduced to simplify the total potential energy summation process. The element stiffness matrix is derived and applied to Newton-Raphson incremental iterative numerical process, and the secant relations are used to minimize the cumulative errors during the numerical iteration process. Besides, the updated Lagrangian method is employed to account for the large deformation issue. Results show that: 1) the proposed method can provide predictions that match well with both the theoretical solutions and field test data; 2) using the pile element model can substantially reduce the number of elements and calculation time compared with those of the discrete element model, and thus significantly improve the calculation efficiency.

Keywords: laterally-loaded piles; finite element method; pile-soil interaction; pile element; multi-layered soils

1 Introduction

At present, laterally-loaded piles are commonly used in infrastructure construction such as highways, bridges and offshore platforms, and they often pass through multi-layered soils. Mechanical analysis of laterally-loaded piles embedded in multi-layered soils is a key step in pile foundation design. The current "*Specifications for design of foundation of highway bridges and culverts* " (JTG 3363-2019)[1] uses the *m* method based on the elastic subgrade reaction method to convert the multi-layered soil scale factor *m* into a uniform soil layer scale factor. However, the physical and mechanical properties of each soil layer are different, and the pile-soil interaction often exhibits highly nonlinear characteristics. Therefore, when the nonlinearity of the local soil is high and the physical and mechanical properties of the soil varies with soil layers, some analysis methods which based on linear elastic theory often produce large errors when analyzing laterally-loaded piles embedded in multi-layered soils. Thus improving the accuracy and calculation efficiency mechanical analysis of laterally-loaded piles embedded in multi-layered soils attract lots of attention in geotechnical engineering[2].

To date, scholars have carried out a series of experimental and theoretical studies on the nonlinear pile-soil interaction in multi-layered soils. The calculation methods can be summarized into the following four categories. (1) Elastic continuum method: In 1973, Poulos[3] assumed that the soil is a continuous linear elastic medium, and proposed an elastic analysis method for analyzing a single pile. Considering that the natural foundation is often a layered structure, Pise[4] derived the theoretical solution of single pile in a two-layer soil system based on the Mindlin solution; Chen et al.[5] improved the Poulos elastic theory by introducing the Mindlin solution of a horizontal concentrated force in the multi-layered soils and improved the accuracy of calculation. However, assumptions based on linear elastic theory limit the scope of application of this method. (2) Elastic subgrade reaction method: This method is mainly divided into *m* method, *K* method, *C* method and constant method[6]. For multi-layered soils, the "*Specifications for design of foundation of highway bridges and culverts*" [1] converts the multi-layered soil scale factor to that of a

Received: 26 November 2020 Revised: 07 April 2021
This work was supported by the National Science Foundation of China (51909288) and the Guangdong Provincial Department of Science and Technology (2019ZT08G090).
First author: ZHAO Hai-peng, male, bore in 1995, Postgraduate student, research interests: design theory and method of foundation engineering. E-mail: zhaohp6@mail2.sysu.edu.cn
Corresponding author: LI Xue-you, male, bore in 1988, Professor, research interests: foundation engineering, computational geotechnical mechanics and reliability theory. E-mail: lixueyou@mail.sysu.edu.cn

uniform soil layer based on the *m* method, and then mechanical analysis of laterally-loaded piles is carried out. However, this method has some problems. Firstly, it ignores the errors caused by the excessive differences in the physical and mechanical properties of different soil layers. Literatures[7−8] pointed out that the difference in mechanical analysis of the surface soil will significantly affect the loading response of the pile. Secondly, the *m* method is an elastic subgrade reaction method, assuming that the surrounding soil is a linear elastic medium, and the lateral resistance of the soil around pile has a linear relationship with the pile deflection. However, the pile-soil interaction shows a linear relationship only when the pile displacement is extremely small. Pile-soil interaction under a larger displacement will show a strong nonlinearity[9−11], and a larger error will occur if the calculation is still based on the linear relationship. (3) Composite foundation reaction method (*p*-*y* method): This method was first proposed by Mcclelland et al.[12], and then Matlock[13] established the *p*-*y* curve of a single pile in saturated soft clay based on field tests. Reese et al.[14] established the *p*-*y* curve of a single pile based on the field test of laterally loaded steel pipe piles in sand and this finding was included in the specification by the American Petroleum Institute (API)[15]. According to the actual situation in China, many studies have been done on the localization and unification of the *p*-*y* curve through field experiments[16-18], model experiments[19-20] and other methods. Compared with the *m* method, the *p*-*y* curve method comprehensively considers the linearity, nonlinearity, delamination, and plastic deformation characteristics of the soil, and can better reflect the pile-soil interaction in the layered soils. Therefore, it is widely used in the mechanical analysis of laterally-loaded piles embedded in multi-layered soils[21−23]. (4) Finite element method: With the development of computer technology, the finite element method is widely used because of its computational efficiency. Among them, the discrete spring element model[1, 24−25] is the most commonly used design method in engineering. As shown in Fig. 1(a), this method uses beam elements and spring elements to simulate piles and the surrounding soil. Since the soil within the length of the beam element is simulated by two discrete springs located at the beam element node (that is, two concentrated forces are used to approximate the continuous distribution of soil resistance within the length of the element). The length of the beam element cannot be too large, otherwise it will cause large errors, especially in the case of different the physical and mechanical properties in the multi-layered soils. To ensure the accuracy of the calculation, a large number of spring elements and beam elements are often required to simulate the surrounding soil and the pile, resulting in difficulty in modelling and inefficient calculation [21].

Therefore, based on the traditional finite element method, this paper proposes a pile element model that can conduct mechanical analysis of laterally-loaded piles embedded in multi-layered soils by considering nonlinear behaviors of the pile-soil interaction. As shown in Fig. 1(b), this method develops a pile element that is different from the traditional beam element and integrates the "soil spring" into the pile element formulations, that is, the pile element comprises both pile and soil properties. Therefore, there is no need to use additional elements to simulate the surrounding soil during modeling, which effectively simplifies the pile−soil system model. In addition, since the surrounding soil within the pile element length is simulated by the distributed springs embedded in the pile element, even if the physical and mechanical properties of the multi-layered soils are very different or the pile-soil interaction is highly nonlinear, the element length will not be subject to excessive restrictions, which can greatly reduce the number of elements and improve calculation efficiency. This article will introduce the derivation and numerical analysis methods of pile elements, and finally verify the accuracy and efficiency of pile elements for analyzing laterally-loaded piles embedded in multi-layered soils through illustrative examples.

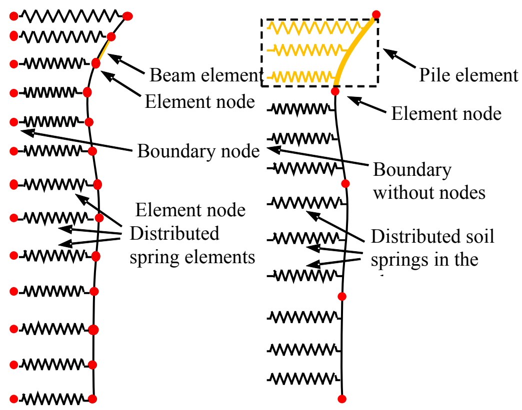

(a) Discrete spring element model (b) Pile element model

Fig. 1 Finite element method

2 Efficient finite element method

2.1 Basic assumptions

In order to simplify the derivation process of the pile element, the following assumptions are adopted: (1) The pile is a flexible pile based on Euler Bernoulli beam theory; (2) Nodal forces are conservative forces; (3) The material of pile body is homogeneous, elastic and isotropic.

2.2 Pile−soil interaction

The $p-y$ method considers the influence of factors such as pile size, soil parameters, and initial modulus of foundation reaction on the elastoplastic properties of the soil. At the same time, it is suitable for flexible piles with pile diameters less than 2 m[13−14]. In this paper, the $p-y$ curve is used to simulate the lateral pile-soil interaction. Take the p-y curve in China's "Code for Pile Foundation of Port Engineering" (JTS 167-4-2012) [26] and API Code[15] as an example.

(1) p-y curve for sand

$$p=\alpha p_{\mathrm{u}}\tanh\left[\frac{kH}{\alpha p_{\mathrm{u}}}\times y\right] \tag{1}$$

where p is the lateral soil resistance; α is the factor to account for static or cyclic loading conditions, $\alpha=[3.0-0.8H/D]\geqslant 0.9$ for static loading, D is the pile diameter; k is the initial modulus of subgrade reaction and it is determined by the angle of internal friction; H is the depth of the soil; p_{u} is the ultimate bearing capacity at depth H, which can be determined using parameters such as soil gravity, internal friction angle and depth; y is the lateral deflection_of the pile at depth H.

(2) p-y curve for clay

$$\left.\begin{aligned} &p=\frac{p_{\mathrm{u}}}{2}\left(\frac{y}{y_{50}}\right)^{\frac{1}{5}},\ y/y_{50}<8 \\ &p=p_{\mathrm{u}},\ y/y_{50}\geqslant 8 \end{aligned}\right\} \tag{2}$$

where $y_{50}=2.5\,\varepsilon_{50}D$, it is the corresponding lateral deflection of the pile when the surrounding soil reaches half of the ultimate lateral soil resistance; ε_{50} is the strain which occurs at one-half the maximum principal stress difference on the triaxial test.

Because ε_{50} is difficult to obtain, Zhang[27] proposed to use the compressibility coefficient a_{v} to express the value:

$$y_{50}=0.015\,8a_{\mathrm{v}}^{1.15}D^{0.75} \tag{3}$$

2.3 Development of pile element

As shown in Fig. 2, a pile with a length of L, a cross-sectional area of A, and a Young's modulus of E is located in the Q-th layer of soil. The thickness of each soil layer is $L_1,\ldots L_q,\ldots L_Q$, and the element length is l. The pile head is subjected to a lateral load of H_0 and a bending moment of M_0. A rectangular axes system X-Y is established with the center O of the pile head as the origin, where the X axis coincides with the center axis of the pile body, the Y axis is parallel to the direction of the lateral load H_0, and the bending moment M_0 acts on the X-Y plane. To simplify the analysis, take one of the pile elements and establish an element local axes system x-y with the center o of the upper part of the pile element as the origin.

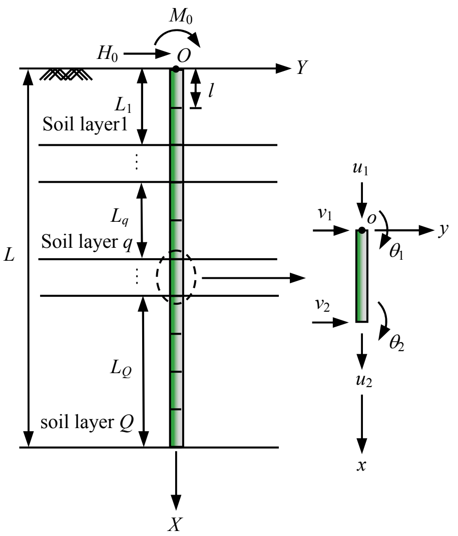

Fig. 2 Model of laterally-loaded pile in multi-layered soils

2.3.1 Element shape function

A one-dimensional shape function is introduced to represent the deformation of the pile element, and the translations and rotations of the nodes are considered, as shown in Fig. 3. The deformation of the element at axial and lateral directions can be described by linear and Hermite interpolation functions, respectively, which can be expressed as

$$\begin{Bmatrix} u(x) \\ v(x) \end{Bmatrix}=\begin{bmatrix} N_1 & 0 & 0 & N_2 & 0 & 0 \\ 0 & N_3 & N_4 & 0 & N_5 & N_6 \end{bmatrix}\begin{Bmatrix} u_1 \\ v_1 \\ \theta_1 \\ u_2 \\ v_2 \\ \theta_2 \end{Bmatrix} \tag{4}$$

where $u(x)$ and $v(x)$ are the displacement functions along the x-axis and y-axis at x position; u_1 and u_2 are the translations along the x-axis at both ends; v_1 and v_2 are the translations along the y-axis at both ends; θ_1, θ_2 are the rotations at both ends; N_1, N_2, N_3, N_4, N_5, and N_6 are the shape function parameters, namely

$$N_1=1-\xi \tag{5}$$

$$N_2=\xi \tag{6}$$

$$N_3 = 1 - 3\xi^2 + 2\xi^3 \tag{7}$$

$$N_4 = \xi l - 2\xi^2 l + \xi^3 l \tag{8}$$

$$N_5 = 3\xi^2 - 2\xi^3 \tag{9}$$

$$N_6 = -\xi^2 l + \xi^3 l \tag{10}$$

where ξ is the normalized coordinate, which is given by

$$\xi = \frac{x}{l} (0 \leqslant \xi \leqslant 1) \tag{11}$$

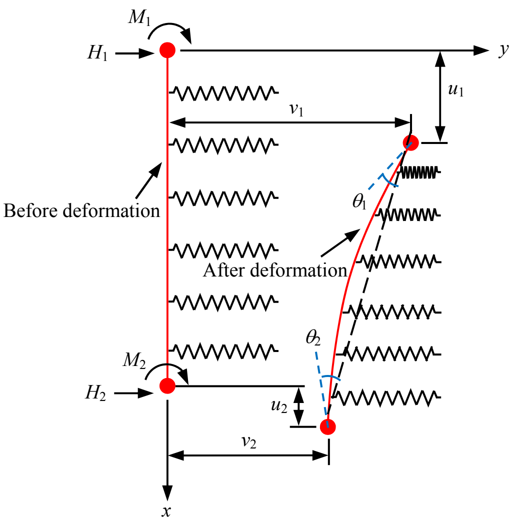

Fig. 3 Forces and deformations of pile element

2.3.2 Total potential energy of the element

The total potential energy J of the pile element can be written as

$$J = J_{\mathrm{E}} + J_{\mathrm{S}} - W \tag{12}$$

where J_{E} is the potential energy of element strain; J_{S} is the potential energy of the distributed soil springs, this term is used to integrate the nonlinear pile-soil interaction into the pile element formula; and W is the work done by external loads. After simplification, the potential energy of element strain is expressed as

$$J_{\mathrm{E}} = \frac{1}{2}\int_0^L \left[EA\left(\frac{\partial u(x)}{\partial x}\right)^2 + EI\left(\frac{\partial^2 v(x)}{\partial x^2}\right)^2 \right] \mathrm{d}x - \int_0^L V\left(\frac{\partial u(x)}{\partial x}\frac{\partial v(x)}{\partial x}\right)\mathrm{d}x + \frac{1}{2}\int_0^L P\left(\frac{\partial v(x)}{\partial x}\right)^2 \mathrm{d}x \tag{13}$$

where I is the moment of inertia; P is element internal force along the element length; V is the shear force.

In the case of multi-layered soils, the p-y curve is generally determined according to the parameters of the pile and each soil layer, and is generally highly nonlinear, so it is difficult to be accurately described with a specific function. Therefore, the Gauss-Legendre method is introduced to compute the potential energy produced by distributed soil springs, which is given by

$$J_{\mathrm{S}} = \int_0^l \int_0^v p\mathrm{d}y\mathrm{d}x = \frac{1}{2}\int_0^l \beta v^2 \mathrm{d}x \approx \frac{1}{2}\sum_{i=1}^n H_i \beta_i v_i^2 \tag{14}$$

where H_i is the weight factor of the i-th Gaussian point; v_i is the lateral translation of the i-th Gaussian point; β_i is the tangent value of the i-th Caussian point along the p-y curve; n is the number of Gaussian points, which is equal to 11 in this paper.

The work done by the external loads is expressed by

$$W = P(u_1 - u_2) + M_1\theta_1 + M_2\theta_2 + V_1 v_1 + V_2 v_2 \tag{15}$$

2.3.3 Element secant stiffness matrix

Nodal force is composed of internal force generated by pile deflection and surrounding soil force. In order to minimize the accumulative error in the incremental iteration process and make the calculation result converge, the secant relationship is introduced to examining the element node force. According to the principle of minimum potential energy, the element balance equation is obtained by the first derivative of Eq. (12).

$$\delta J = \frac{\partial J}{\partial u_i} + \frac{\partial J}{\partial F_i}\frac{\partial F_i}{\partial u_i} = 0 \tag{16}$$

where u_i represents the i-th degree of freedom; F_i is the corresponding nodal force.

2.3.4 Element tangent stiffness matrix

In FEA, the element tangent stiffness matrix is established to predict the displacements on the elements nodes. And the element tangent stiffness matrix is obtained by the second derivative of Eq. (12)

$$\delta^2 J = \frac{\partial^2 J_i}{\partial u_i \partial u_j}\delta u_i \delta u_j \tag{17}$$

Since the soil properties are directly considered in the pile element, the element tangent stiffness matrix is composed of 3 parts, namely

$$[k]_{\mathrm{E}} = [k]_{\mathrm{L}} + [k]_{\mathrm{G}} + [k]_{\mathrm{S}} \tag{18}$$

where $[k]_{\mathrm{L}}$ is the linear stiffness matrix; $[k]_{\mathrm{G}}$ is the geometric stiffness matrix; $[k]_{\mathrm{S}}$ is the soil stiffness matrix. Each stiffness matrix is expressed as follows:

$$[k]_{\mathrm{L}}=\begin{bmatrix} \dfrac{EA}{l} & 0 & 0 & -\dfrac{EA}{l} & 0 & 0 \\ & \dfrac{12EI}{l^3} & \dfrac{6EI}{l^2} & 0 & -\dfrac{12EI}{l^3} & \dfrac{6EI}{l^2} \\ & & \dfrac{4EI}{l} & 0 & -\dfrac{6EI}{l^2} & \dfrac{2EI}{l} \\ & & & \dfrac{EA}{l} & 0 & 0 \\ & \text{Symmetry} & & & \dfrac{12EI}{l^3} & -\dfrac{6EI}{l^2} \\ & & & & & \dfrac{4EI}{l} \end{bmatrix} \tag{19}$$

$$[k]_{\mathrm{G}}=\begin{bmatrix} \dfrac{P}{l} & -\dfrac{M_1+M_2}{l^2} & 0 & -\dfrac{P}{l} & \dfrac{M_1+M_2}{l^2} & 0 \\ & \dfrac{6P}{5l} & \dfrac{P}{10} & \dfrac{M_1+M_2}{l^2} & -\dfrac{6P}{5l} & \dfrac{P}{10} \\ & & \dfrac{2lP}{15} & 0 & -\dfrac{P}{10} & -\dfrac{lP}{30} \\ & & & \dfrac{P}{l} & -\dfrac{M_1+M_2}{l^2} & 0 \\ & \text{Symmetry} & & & \dfrac{6P}{5l} & -\dfrac{P}{10} \\ & & & & & \dfrac{2lP}{15} \end{bmatrix} \tag{20}$$

$$[k]_{\mathrm{S}}=\begin{bmatrix} 0 & 0 & 0 & 0 & 0 & 0 \\ & \sum_{i=1}^{n}\alpha_{1i}\beta_i l & \sum_{i=1}^{n}\alpha_{2i}\beta_i l^2 & 0 & \sum_{i=1}^{n}\alpha_{3i}\beta_i l & \sum_{i=1}^{n}\alpha_{4i}\beta_i l^2 \\ & & \sum_{i=1}^{n}\alpha_{5i}\beta_i l^3 & 0 & \sum_{i=1}^{n}\alpha_{6i}\beta_i l^2 & \sum_{i=1}^{n}\alpha_{7i}\beta_i l^3 \\ & & & 0 & 0 & 0 \\ & \text{Symmetry} & & & \sum_{i=1}^{n}\alpha_{8i}\beta_i l & \sum_{i=1}^{n}\alpha_{9i}\beta_i l^2 \\ & & & & & \sum_{i=1}^{n}\alpha_{10i}\beta_i l^3 \end{bmatrix} \tag{21}$$

where the integration coefficients α_{1i} to α_{10i} are from literature [21].

2.4 Numerical method

The non-linear finite element numerical analysis process based on pile elements has been implemented by self-programming in Python language. Considering that laterally-loaded piles often exhibit large deformations in soft soils[28], the updated Lagrangian method[21] is employed to account for the large deformation issue, and the equilibrium conditions are established to iterate based on the known element states in the previous step.

In the case of multi-layered soils, the internal friction angle, cohesion, gravity and other parameters of each soil layer are apparently different significantly affect the interaction between the soil layers and the pile-soil system. That is, the $p-y$ curve has obvious stratification according to the parameters of each soil layer, as shown in Fig. 4.

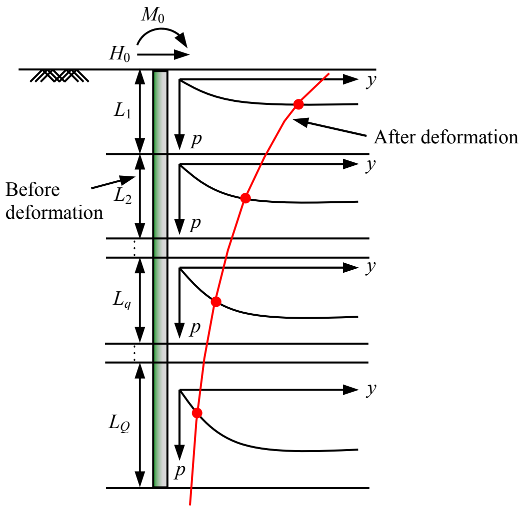

Fig. 4 $p-y$ curves of each soil layer along the pile length

From this, the stiffness matrix of each soil layer is derived, namely

$$\begin{aligned} [K]_1 &= \sum_{t=1}^{t_1}\Big([B]_t\big([k]_{\mathrm{L}}+[k]_{\mathrm{G}}+[k]_{\mathrm{S1}t}\big)[B]_t^{\mathrm{T}}\Big) \\ [K]_2 &= \sum_{t=1}^{t_2}\Big([B]_t\big([k]_{\mathrm{L}}+[k]_{\mathrm{G}}+[k]_{\mathrm{S2}t}\big)[B]_t^{\mathrm{T}}\Big) \\ &\cdots \\ [K]_q &= \sum_{t=1}^{t_q}\Big([B]_t\big([k]_{\mathrm{L}}+[k]_{\mathrm{G}}+[k]_{\mathrm{S}qt}\big)[B]_t^{\mathrm{T}}\Big) \\ &\cdots \\ [K]_Q &= \sum_{t=1}^{t_Q}\Big([B]_t\big([k]_{\mathrm{L}}+[k]_{\mathrm{G}}+[k]_{\mathrm{S}Qt}\big)[B]_t^{\mathrm{T}}\Big) \end{aligned} \tag{22}$$

where $[K]_q$ is the stiffness matrix of the q-th soil layer; $[B]_t$ is the transposed matrix of the t-th element[29]; t_q is the number of elements of the q-th soil layer; $[k]_{\mathrm{S}qt}$ is the stiffness matrix of the t-th element of the q-th soil layer that reflects the soil properties.

After assembling the stiffness matrix of each soil layer in order, the global stiffness matrix $[K]$ is obtained

$$[K]=\sum_{q=1}^{Q}[K]_q \tag{23}$$

The Newton-Raphson incremental iterative procedure is employed. First, the external load is divided into specified load steps for incremental application (the same incremental load is applied for each load step), and then the equilibrium condition is established according to the secant relationship and the unbalanced force is solved. Finally, the convergence criterion is used to determine whether the requirements are met, and judge whether it is necessary to continue incremental iterations. If the current step is the m-th iteration of the n-th load step, the incremental iteration process is as follows:

Based on the global stiffness matrix, the incremental nodal displacement vector in the global axis system is calculated, namely

$$\{\Delta U\}_m = \begin{cases} \{\Delta F\}[K]^{-1} & , m = 1 \\ \{\Delta F'\}_m [K]^{-1} & , m \geqslant 2 \end{cases} \tag{24}$$

where $\{\Delta U\}_m$ is the incremental nodal displacement vector in the m-th step; $\{\Delta F\}$ is the incremental force vector applied in the n-th load step; $\{\Delta F'\}_m$ is the unbalanced force vector generated in the m-th step.

The total incremental nodal displacement is calculated by the following formula, namely

$$\{U\}_m = \sum_{m=1}^{\mathrm{NEM1}} \{\Delta U\}_m \tag{25}$$

where $\{U\}_m$ is the total incremental nodal displacement in the m-th step; and NEM1 is the current step.

The incremental nodal displacement vector $\{\Delta u\}_t$ in the element local axis system can be calculated by the following formula, namely

$$\{\Delta u\}_t = [B]_t \{\Delta U\}_t \tag{26}$$

where $\{\Delta u\}_t$ is the incremental nodal displacement of the t-th element in the local axis system; and $\{\Delta U\}_t$ is the incremental nodal displacement of the t-th element in the global axis system.

After obtaining the incremental nodal displacement, it is substituted into the secant relationship to calculate the incremental element resistance vector$\{\Delta R\}_t$, and assembled into the global incremental resistance vector, the total resistance vector at the m-th step is given by

$$\{R\}_m = \{R\}_{m-1} + \sum_{t=1}^{\mathrm{NELE}} [B]_t^{\mathrm{T}} \{\Delta R\}_t \tag{27}$$

where $\{R\}_m$ is the total incremental resistance vector at the m-th step; $\{\Delta R\}_t$ is the soil incremental resistance vector of the t-th element; NELE represents the number of the elements.

The total load applied by the corresponding load step can be calculated according to the following formula, namely

$$\{F\}_n = \sum_{n=1}^{\mathrm{NEM2}} \{\Delta F\} \tag{28}$$

where $\{F\}_n$ is the total load vector applied at the n-th load step; NEM2 is the current load step.

After obtaining the total resistance vector at the m-th step and the total applied load, the unbalanced force vector can be calculated as follows:

$$\{\Delta F'\}_m = \{F\}_n - \{R\}_m \tag{29}$$

Finally, the following convergence criterion is used to determine whether the iteration has converged, that is

$$\frac{\{\Delta U\}_m^{\mathrm{T}} \{\Delta U\}_m}{\{U\}_m^{\mathrm{T}} \{U\}_m} \leqslant T \tag{30}$$

$$\frac{\{\Delta F'\}_m^{\mathrm{T}} \{\Delta F'\}_m}{\{R\}_m^{\mathrm{T}} \{R\}_m} \leqslant T \tag{31}$$

where T is the convergence value.

After m times iterations, judge whether the iteration meets the requirements according to the convergence criterion. If it is satisfied, the incremental iterative process of load step n+1 is carried out; otherwise the unbalanced force is used as an applied external loads to act on the system until the convergence criterion is satisfied.

3 Illustrative example

3.1 Linear pile−soil interaction

The pile−soil interface satisfies the linear elastic assumption under the condition of small deformation, and the problem of laterally-loaded piles embedded in multi-layered soils has an theoretical solution. The following example is used to verify the accuracy and efficiency of the pile element model under the linear elastic condition. As shown in Fig. 5, consider a circular cross-section cast-in-place pile[30], the pile diameter D= 1 m, the Young's modulus of the pile E=32.35 GPa. A lateral load of 150 kN is applied on the pile head, the pile head is free and the pile toe is fixed. The surrounding soil has two layers, the upper layer is a flow-plastic backfill with a thickness of 2 m, the scale factor m_1= 3 000 kN/m^4, and the lower layer is a hard plastic cohesive soil with a thickness of 10 m, the scale factor m_2=20 000 kN/m^4.

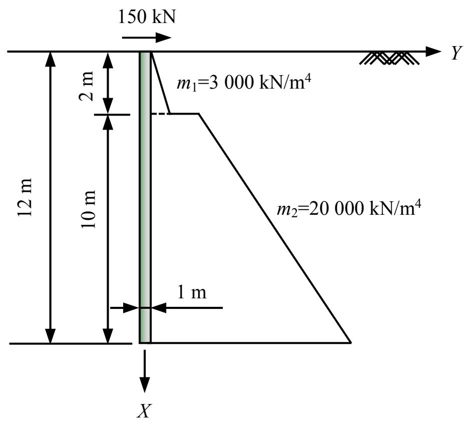

Fig. 5 Diagram of the pile−soil system

Lateral displacement of the pile head and the maximum bending moment at 3 m below the pile head are simulated by the m method, pile element model, and discrete spring element model. The comparative results between the predicted results and the theoretical solution are shown in Table 1. The results of the discrete spring element model are calculated by the finite element analysis software NIDA [31], and the calculation time is obtained by a computer with an Intel(R) Core(TM) i5-7200 processor and 8 GB memory. Table 1 illustrates that the m method based on the conversion of multi-layered soils area is very different from the theoretical solution in predicting the displacement and bending moment of the pile. The improved m method based on the weighted conversion of the multi-layered soils deflection curve still has a big error. The error of the discrete spring element model decreases as the number of elements increases. When the total number of elements is 89 (45 beam elements and 44 spring elements), the results match well with the theoretical solution. While the pile element model can accurately predict the displacement and bending moment of the pile with only 15 elements. From the prospect of calculation time, in order to achieve the same calculation accuracy as the theoretical solution, the discrete spring element model took 10.2 s, while the pile element model only took 0.4 s, which greatly reduced the calculation time. This is because the number of elements directly determines the size of the stiffness matrix, which affects the computational complexity of the finite element (see Eq. (24)). Compared with the discrete spring element model, the pile element model greatly reduces the number of elements (about 6 times) with the same accuracy, thereby reducing the dimension of the stiffness matrix and improving the overall calculation efficiency. Considering that actual projects often involve dozens or even hundreds of piles, when the integrated analysis of these piles is required, the computational efficiency advantage brought by the small number of element used in the pile element model will be more prominent.

Table 1 Predicted results and relative errors

Calculation method	Element number	Pile head displacement /mm	Relative error /%	Maximum bending moment /(kN • m)	Relatively Error /%	Calculation time /s
Analytical solution [30]	—	4.373 5	—	336.81	—	—
m Method-1[30]	—	3.015 6	−31.05	238.95	−29.05	—
m Method-2[30]	—	4.209 3	−3.75	343.83	2.08	—
	29	5.053 6	15.55	381.45	13.25	6.2
Discrete spring element model	59	4.450 3	1.76	348.21	3.38	7.4
	89	4.371 7	−0.04	343.35	1.94	10.2
Pile element model	15	4.372 4	−0.03	343.62	2.02	0.4

Note: *m* method-1 is the *m* method based on the conversion of multi-layered soil area; *m* method-2 is the *m* method based on weighted conversion of the multi-layered soils deflection curve.

3.2 Nonlinear pile−soil interaction

In actual engineering, the soil layer is often complex and highly nonlinear. In this example, a test pile[32] in the suburbs of Shanghai is selected for analysis. As shown in Fig. 6, the test pile is a steel pipe pile with a pile diameter of 0.5 m, a pile depth of 13.28 m, and a free height of 0.72 m. The bending rigidity of the pile is 97 939.67 kN·m^2. The geotechnical parameters of the test site are shown in Table 2. The test is divided into two groups: the pile head of group a is subjected to lateral load H_0=60.055 5 kN; the pile head of group b is subjected to lateral load H_0=80.078 4 kN. This calculation example uses the empirical formula for calculating the *p-y* curve of clay proposed in the literature [27], which uses field test parameters to calculate the *p-y* curve of each soil layer, as shown in Fig. 7. The pile element model and the discrete spring element model are respectively used for calculating the lateral displacement and bending moment of the pile along the depth distribution, as shown in Figs. 8 and 9.

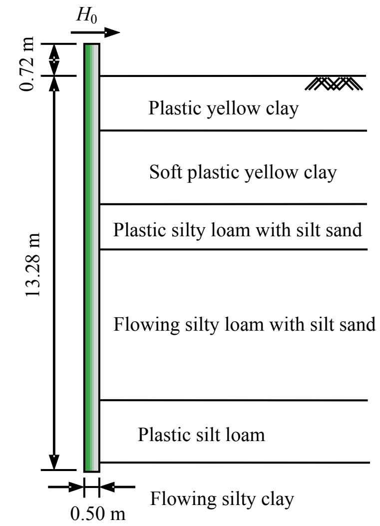

Fig. 6 Geological profile of the test site

Table 2 Soil properties of the test site[27]

Embedded depth /m	Soil layer	C /kPa	φ /(°)	γ' /(kN • m^{-3})	a_v /MPa^{-1}
0−1.5	Plastic yellow clay	34	4.0	8.9	0.51
1.5−4.4	Soft plastic yellow clay	13	1.0	7.1	0.86
4.4−5.5	Plastic silty loam with silt sand	51	3.5	9.0	0.10
5.5−11.0	Flowing silty loam with silt sand	13	4.5	7.1	0.51
11.0−13.0	Plastic silt loam	24	2.5	7.9	0.66
13.0−15.4	Flowing silty clay	10	1.5	7.1	1.14

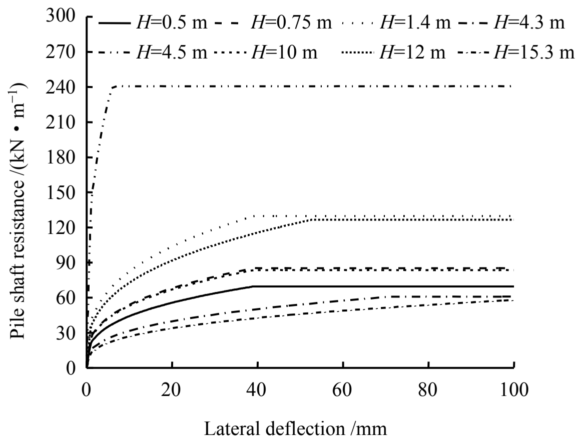

Fig. 7 *p-y* curves of each soil layer

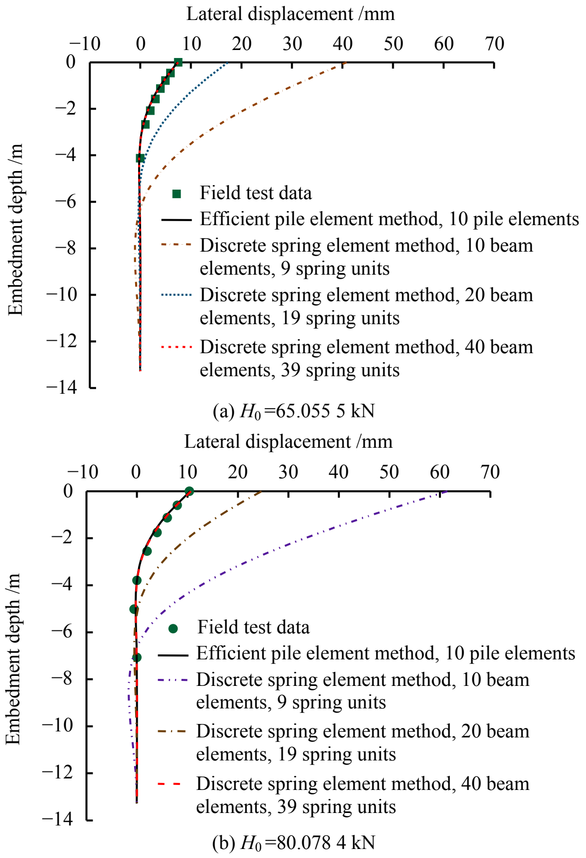

Fig. 8 Depth−lateral displacement curves of pile

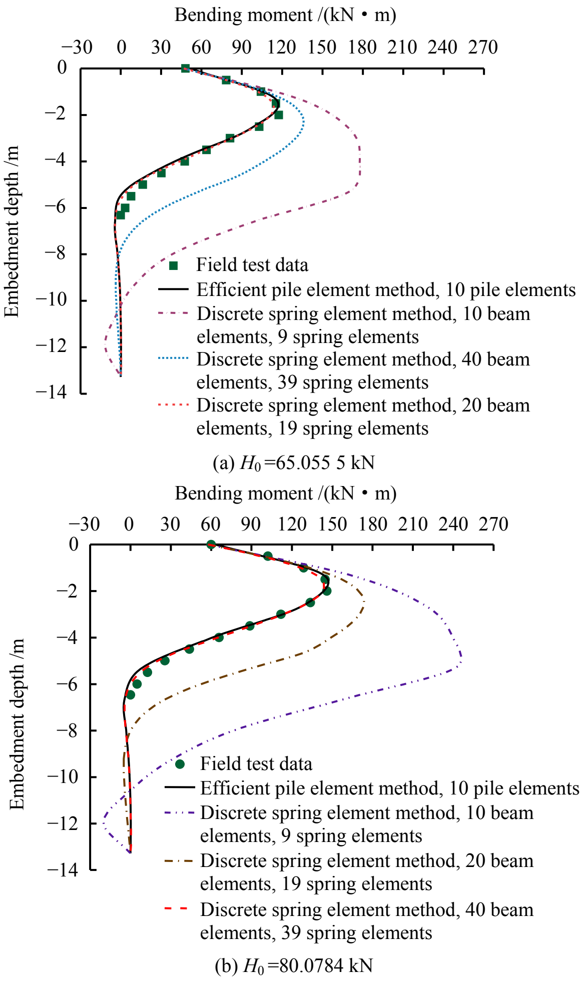

Fig. 9 Depth−bending moment curves of pile

Figures 8 and 9 illustrate that the pile element model with 10 pile elements match well with the field test data in simulating the lateral displacement and bending moment which validates the accuracy of the pile element model under the condition of complex soil layer and the nonlinear soil properties. The discrete spring element model requires at least 79 elements (40 beam elements and 39 spring elements) to achieve the same accuracy, which is about 8 times the number of elements in the proposed method. For reaching the same accuracy with the field test data, the discrete spring element model took 9.5 s, while the pile element model took only 0.45 s. It is thus clear that the pile element model can substantially reduce the number of elements and calculation time than in the case of linear elasticity, when considering the nonlinear pile-soil interaction.

4 Conclusion

(1) This paper develops a pile element model suitable for analyzing laterally-loaded piles embedded in multi-layered soils. The element is incorporated with a distributed "soil spring" to consider the properties of the soil and combined with the $p-y$ method to consider the nonlinear pile-soil interaction. The tangent stiffness matrix of each soil layer is derived in this paper and it is assembled to form the global stiffness matrix, which is used to calculate the displacement in the Newton-Raphson incremental iteration, and the convergence of the iteration is achieved through the secant relationship.

(2) The calculation example shows that the pile element model is accurate and efficient when analyzing laterally-loaded piles embedded in multi-layered soils. Under the conditions of linear and nonlinear behaviors of pile−soil interaction, fewer elements and shorter calculation time are used in the pile element model than those in the discrete spring element model to accurately predict the pile displacement and bending moment of the laterally loaded pile. It is more accurate than the m method recommended in "*Specifications for design of foundation of highway bridges and culverts*".

References

[1] CCCC Highway Consultants Limited Company. JTG 3363—2019 Specifications for design of foundation of highway bridges and culverts[S]. Beijing: China Communications Press, 2019.

[2] DAI Zi-hang, WANG Yun-feng, LU Cai-jin. Numerical solution of link finite element based on composite stiffness and bi-parameter method for computation of laterally loaded single pile[J]. Chinese Journal of Rock Mechanics and Engineering, 2016, 35(10): 2115−2123.

[3] POULOS H G. Analysis of piles in soil undergoing lateral movement[J]. Journal of the Soil Mechanics and Foundations Division, 1973, 99(5): 391−406.

[4] PISE P J. Laterally loaded piles in a two-layer soil system[J]. Journal of the Geotechnical Engineering Division, 1982, 108(9): 1177−1181.

[5] CHEN Fu-quan, HUANG Wei-da. A modified analysis method for passive pile based on Poulos's elastic theory[J]. Rock and Soil Mechanics, 2008, 29(4): 905−910.

[6] ZHAO Ming-hua. Analysis of pile under multi-layer foundation and lateral load[J]. Central South Highway Engineering, 1986(4): 54−60.

[7] ZHANG Wang-xi, ZHAN Xin-jie, YI Wei-jian, et al. Solution to the lateral displacement of lateral loaded long-piles under double-parameter layered-foundation[J]. Journal of Hunan University (Natural Sciences), 2011, 38(3): 17−21.

[8] ZHANG L, ZHAO M, ZOU X. Behavior of laterally loaded piles in multilayered soils[J]. International Journal of Geomechanics, 2015, 15(2): 06014017.

[9] WANG Hao-tian, DONG Sheng. Comparative study on full-structure segment and single-row models of high-pile wharves based on the *p-y* curve method[J]. Engineering Mechanics, 2019, 36(Suppl. l): 278−284.

[10] YIN Ping-bao, NIE Dao-liu, YANG Zhao-hui, et al. The *p-y* curve and computation method of the horizontal bearing capacity of piles in sloping ground[J]. Chinese Journal of Rock Mechanics and Engineering, 2018, 37(4): 996−1003.

[11] YAN Bin. Study on simplified models of bridge pile-foundation subjected to earthquake[D]. Shanghai: School of Civil Engineering, Tongji University, 2007: 66−68.

[12] MCCLELLAND B, FOCHT J A. Soil modulus for laterally loaded piles[J]. Journal of the Soil Mechanics and Foundations Division, 1956, 82(4): 1−22.

[13] MATLOCK H. Correlation for design of laterally loaded pile in soft clay[C]//Proceedings of 2nd Offshore Technology Conference. Houston: [s. n.], 1970: 577−594.

[14] REESE L C, COX W R, KOOP F D. Field testing and analysis of laterally loaded piles in stiff clay[C]// Proceedings of 7nd Offshore Technology Conference. Houston: [s. n.], 1974: 473−483.

[15] American Petroleum Institute. Recommended practice for planning, designing, and constructing fixed offshore platforms-working stress design[M]. Washington D C: [s. n.], 2002.

[16] GE Xun, ZHAO Qi-hua, XUE Qiu-chi. Interaction of pile-soil in horizontal loaded piles[J]. Journal of Water Resources and Architectural Engineering, 2008, 16(1): 36−39+47.

[17] LI Hong-jiang, TONG Li-yuan, LIU Song-yu, et al. Parameter sensitivity of horizontal bearing capacity of large diameter and super-long bored pile[J]. Rock and Soil Mechanics, 2008, 39(5): 1825−1833.

[18] LI H J, TONG L Y, LIU S Y. Effect of excavation unloading on *p-y* curves for laterally loaded piles[J]. Computers and Geotechnics, 2018, 104: 131−139.

[19] WANG Xiao-wei, YE Ai-jun, SHANG Yu. Shallow-layer *p-y* curves for single micropile in sands[J]. Chinese Journal of Geotechnical Engineering, 2008, 40(9): 1736−1745.

[20] WOO K S, LEE D W, AHN J S. Impact behavior of a laterally loaded guardrail post near slopes by hybrid sph model[J]. Advances in Civil Engineering, 2018(PT.6): 9479452.1-9479452.12.

[21] LI X Y, WAN J H, LIU S W, et al. Numerical formulation and implementation of Euler-Bernoulli pile elements considering soil-structure-interaction responses[J]. International Journal for Numerical and Analytical Methods in Geomechanics, 2020, 44: 1903−1925.

[22] CAO Wei-ping, XIA Bing, GE Xin. Formation and application of hyperbolic *p-y* curves for horizontally loaded single batter piles[J]. Journal of Zhejiang University (Engineering Science), 2019, 53(10): 1946−1954.

[23] YU Shi-zhang, LI Sa. *p-y* curve methods of steel pipe pile foundations under combined loads[J]. Journal of Hydroelectric Engineering, 2008, 37(1): 101−109.

[24] RAHMANI A, TAIEBAT M, FINN W D L, et al. Evaluation of *p-y* springs for nonlinear static and seismic soil-pile interaction analysis under lateral loading[J]. Soil Dynamics and Earthquake Engineering, 2018, 115: 438−447.

[25] ZHANG X, TANG L, LI X, et al. Effect of the combined action of lateral load and axial load on the pile instability in liquefiable soils[J]. Engineering Structures, 2020, 205: 110074.

[26] CCCC Third Harbor Consultants Limited Company. JTS 167-4 — 2012 Code for pile foundation of Harbor Engineering[S]. Beijing: China Architecture and Building Press, 2012.

[27] ZHANG Shu-yu. Study on *P-Y* curves of laterally loaded pile under static loading[D]. Nanjing: School of Transportation and Ocean Engineering, Hohai University, 2001: 36−37+39.

[28] DENG Tao, LIN Cong-yu, LIU Zhi-peng, et al. A simplified elastoplastic method for laterally loaded single pile with large displacement[J]. Rock and Soil Mechanics, 2020, 41(1): 95−102.

[29] LIU S W, LIU Y P, CHAN S L. Direct analysis by an arbitrarily-located-plastic-hinge element — part 2: spatial analysis[J]. Journal of Constructional Steel Research, 2014, 103: 316−326.

[30] DAI Zi-hang, CHEN Lin-jing. Two numerical solutions of laterally loaded piles installed in multi-layered soils by *m* method[J]. Chinese Journal of Geotechnical Engineering, 2007, 29(5): 690−696.

[31] NIDA Professional 10. User manual of Nida professional 10[M]. Guangzhou: Nida Technology Co. Ltd., 2018.

[32] Teaching and Research Office of Harbor Engineering, Hohai University. *P-Y* curve test analysis report of laterally loaded pile in soft clay[R]. Nanjing: Teaching and Research Office of Harbor Engineering, Hohai University, 1986.